CHEMICAL ENGINEERING TRANSACTIONS
VOL. 108, 2024
A publication of AIDIC
The Italian Association of Chemical Engineering
Online at www.cetjournal.it
Guest Editors: Carlo Pirola, Antonio Espuña

ISBN 979-12-81206-08-3; **ISSN** 2283-9216
DOI: 10.3303/CET24108008

Multi-scale Simulations in a Catalytic Reactor Considering Three-Dimensional Pellet Geometry

Yoichi Takagishi*, Ryohei Baba, Takeshi Yamashita, Wataru Adachi

Computational Science Center, Kobelco Research Institute Inc., 1-1-5, Takatsukadai, Nishi-ku, Kobe, 651-2271, Japan
takagishi.yoichi@kki.kobelco.com

Catalytic reactors that convert carbon dioxide into methanol are one of the key technologies in carbon recycling. Various numerical simulations have been conducted to study catalytic reactors, including multi-step chemical reactions, flow, reaction heat, heat transfer, and diffusion. However, in most cases, the microstructures of the catalyst bed are treated as a homogeneous body, in which permeability, diffusion coefficient, and thermal conductivity are estimated by simplified estimation formula, making it difficult to evaluate the effects of the differences in pellet shapes. In this study, we developed a macroscopic homogenization model combined with a three-dimensional microstructure in the catalyst bed in order to predict complex phenomena in the reactor. The model validation was also performed with the actual experiments of catalytic reactions. Furthermore, the effects of different pellet shapes on the temperature, flow field, and reaction field in the reactor were compared.

1. Introduction

CO_2 methanation through conversion into fuels and chemicals such as methane or methanol is recognized as a key technology for “carbon recycling” (Kato et al., 2010). The efficiency of the conversion reactions strongly depends on both macro and microscopic factors. The former includes the catalytic performance and pellet shape, etc., and the latter includes reactor geometry, heating conditions, inward gas pressure etc. (Zhang, 2021). Computational fluid dynamics (CFD) have been adopted widely for use in macroscopic simulations, which provide various information regarding gas flow velocity components, pressure, temperature, and chemical species concentration in a reactor. The most used models assume the fixed bed to be the homogeneous media, represented by porosity, specific surface area, and effective material properties, including permeability and thermal conductivity. In addition to simple one-dimensional models (An, 2017), two- (Adji et al., 2019), and three-dimensional models (Son et al., 2019) have been developed with the various kinetic reaction models. Although these models have advantages in computation efficiency, they present some difficulties when considering the effect of the actual non-uniformity of a packed bed. Recently, particle-resolved CFD simulations, which consider the 3D-packed structure of the catalyst pellets, have been reported (Maestri et al., 2013; Dixon et al., 2019). Nevertheless, such realistic 3D models require large-scale calculation costs.
In this study, a stepwise multiscale model of a fixed-bed CO_2 methanation reactor was developed considering the effect of 3D-packed pellet geometry. The key idea of this approach is that the effective properties, including porosity, specific surface area, etc., are evaluated by the particle-resolved model and used for the homogeneous reactor model. The model validation was conducted with the methanol synthesis experiment for cylindrical pellets of $Zn.Al_2O_3$. Moreover, the effects of pellet shapes on the reactor’s performance were discussed.

2. Model Development

2.1 Flow of stepwise multi-scale simulations

The flow of this study is as follows (Fig.1). Firstly, a particle-resolved 3D-packed structure of the catalyst pellets (micro-scale model) was developed, and the effective properties, including porosity, specific surface area, permeability, and thermal conductivity, were evaluated. Next, a 2D axial symmetric homogeneous multi-physics model (macro-scale model) was constructed, in which the effective properties in the catalyst bed were the values

Paper Received: 04 December 2023 ; Revised: 21 December 2023 ; Accepted: 19 January 2024
Please cite this article as: Takagishi Y., Baba R., Yamashita T., Adachi W., 2024, Multi-scale Simulations in a Catalytic Reactor Considering Three-dimensional Pellet Geometry, Chemical Engineering Transactions, 108, 43-48 DOI:10.3303/CET24108008

obtained from the above model, in order to simulate the reaction, gas flow, pressure, and temperature fields in the reactor. Next, a methanol synthesis experiment was conducted, and the micro-scale model was validated. Finally, micro-scale simulations with different pellet shapes were also carried out, and the reactor's performance was predicted by the macro-scale model. GeoDict 2020 and COMSOL Multiphysics™ ver.5.6 were adopted for the micro-scale simulation and the macro-scale simulation, respectively.

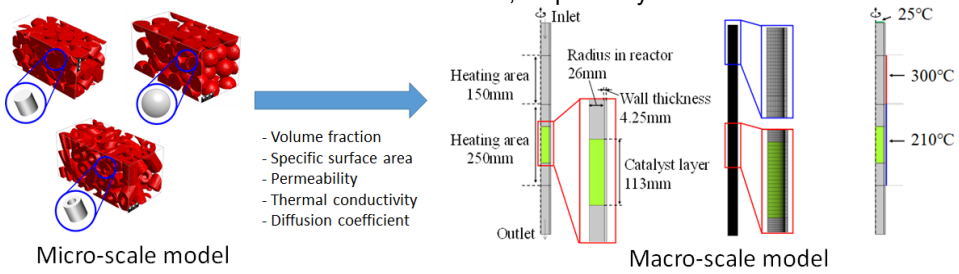

Figure 1. Flow of model development and validation.

2.2 Simulation method of micro-scale model

In the micro-scale model, the 3D random-packed structure of the catalyst pellets is constructed first, and the porosity and the specific surface area are estimated. Herein, the cylinder, sphere and hollow cylinder were adopted as typical pellet shapes (Table.1). The pellets were piled randomly in the larger simulation box with the point contact condition, and the edge regions within the pellet size were cropped. Next, the gas flow, the diffusion of the chemical species, and the heat transfer simulations were conducted separately for evaluation of the permeability and the effective thermal conductivity, respectively. Navier–Stokes and mass conservation equations were used for the evaluation of the gas flow field and the pressure in the reactor. The constant gas pressure 1 Pa was applied to the inlet boundary and the zero-pressure condition was used in the outlet boundary opposite to the inlet boundary. The permeability κ_{micro} of the gas flow in the micro-scale is estimated by

$$\kappa = \mu u_{ave}(dp/dx)^{-1} \quad (1)$$

where μ, u_{ave}, and x represent the viscosity, the average flow velocity, and the position of the main flow direction, respectively. The effective diffusion coefficient of the species was evaluated based on mass conservation law,

$$\nabla \cdot (D_i \nabla c_i) = 0, \quad D_{eff,i} = -j_{ave,i}(dc/dx)^{-1} \quad (2)$$

where *c* and *D* represent the concentration and the diffusion coefficient, respectively. The suffix *i* indicates the species number (i=1, 2, 3 correspond to CO_2, H_2, and CH_3OH, respectively). $j_{ave,i}$ is the average heat flux for the direction from the inlet to the outlet boundary. Note that the diffusion simulation was conducted in the pore (gas) region of the micro-scale model.

Table 1. Properties of the gas and catalyst bed used in this study

	Pellet catalyst	CO_2	H_2
Density (kg/m^3])	2781	1.42	0.063
Viscosity (Pa*s)	-	2.15×10^{-5}	2.15×10^{-5}
Specific heat (J/kg)	1000	919	14470
Thermal conductivity (W/(m^2*K))	1.0	0.022	0.23

2.3 Simulation method of macro-scale model

The macro-scale 2D axial symmetric homogeneous models were constructed in order to simulate the reaction, gas flow, pressure, and temperature fields in the reactor. The parameters, including the effective properties in the catalyst bed, were based on the values obtained by the micro-scale model described in 2.2. The dimensions of the reactor and the catalyst bed layer were set to the same values as in the actual experiment (see in 2.4). The boundary conditions of the reactor are also shown in Fig.1.

As the governing equations for the gas phase in the reactor, the momentum conservation law, mass conservation law, reaction equations, and heat transfer equation were used. The Brinkman equation based on the Darcy velocity and pressure, and the mass conservation law in the porous material were adopted (Alarcon et al., 2022) using the estimated effective permeability and the porosity in the micro-scale model.

Although the following overall reactions of CO_2 methanation (3)-(5) were proposed typically, the reactions related to CO (eq.(4)) are omitted for simplicity (Taco-Vasquez et al., 2022) in this study.

$$CO_2 + 3H_2 \rightleftarrows CH_3OH + H_2O \quad (3)$$

$$CO + 2H_2 \rightleftarrows CH_3OH \quad (4)$$

$$CO_2 + H_2 \rightleftarrows CO + H_2O \quad (5)$$

The simplified kinetic model of methanol synthesis can be described as

$$r = k^f[CO_2][H_2]^3 - k^r[CH_3OH] \quad (6)$$

where k_f, k_r indicate the reaction rate constant for CH_3OH generation and decomposition, respectively. Both rate constants are assumed to follow the Arrhenius form.

$$k^f = A^f\left(T/T_{ref}\right)\exp\left(-E^f/R_gT\right), \quad k^r = A^r\left(T/T_{ref}\right)\exp\left(-E^r/R_gT\right) \quad (7)$$

where T and T_{ref} indicate the temperature in the reactor and the reference temperature, respectively. Herein, the pre-factor value of A_f, and A_r is adopted as 35 $(mol^4\ s)^{-1}$ and 0.0035 $(mol\ s)^{-1}$, and 58700 J/mol was used for the activation energy both E_f and E_r. Due to the simplicity of this model, direct comparison with previously studies using the typical Vanden Bussche and Froment model (Shahrokhi et al., 2005) is not feasible. However, the values of the activation energies are similar. The species of CO_2, H_2 and CH_3OH concentrations in each time were simulated based on the time-dependent mass transportation equation with the convection term

$$\frac{\partial c_i}{\partial t} = \nabla\cdot(D_i\nabla c_i) + u\cdot\nabla c_i + R_i, \quad \rho C_p\frac{\partial T}{\partial t} = \nabla\cdot(k\nabla T) + u\cdot k\nabla T \quad (8)$$

where R_i represents the reaction rate. The temperature in the gas phase and the catalyst bed were evaluated by the heat transfer equation.

2.4 Experimental method of methanol synthesis

The methanol synthesis experiments with a fixed catalyst bed were conducted in order to validate the macro-scale model. Figure 2 illustrates the experimental set up. A quartz tube reactor with an internal diameter of 26 mm and 4.25 mm thickness was used, and $Zn.Al_2O_3$ tablet catalysts were placed in the middle of the reactor tube. The dry CO_2 and H_2 gases were fed by two mass flow controllers (MFC) with the ratio of CO_2:H_2 = 8:2, and the pressure in the reactor was maintained at 0.4 MPa-G. The reactor was heated to 210 ℃ from the periphery by the electrical heating wires. The gas temperature was monitored at the upper surface, the middle of the catalyst layer, and the lower position in the reaction tube (below the catalyst layer). After passing through the catalyst layer, the gas was recovered and the CH_3OH concentration was analysed. The experiments consisted of the following steps: as the first step, a cold-case experiment (without reaction) was conducted in order to validate the micro-scale parameters estimated in the micro-scale simulation, and the methanol synthesis experiments were carried out to validate the macro-scale model.

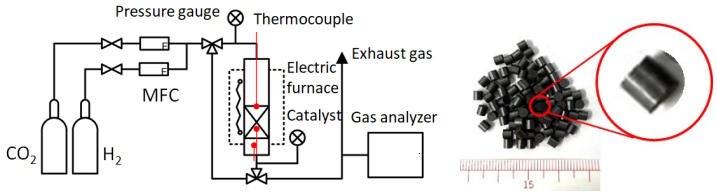

Figure 2. Experimental set up in this study.

3. Results

3.1 Model validation

The permeability, effective diffusion coefficient, and effective thermal conductivity of the catalyst beds with cylindrical pellet geometries were estimated using the particle-resolved micro-scale model. Figure 3 shows the steady-state pressure, concentration distribution of the gas phase, and the temperature distribution. Each gradient is formed from the inlet to outlet boundary through the pore region. The volume fraction of the pellets, the specific surface area, and the estimated permeability by eq.(1) are listed in Table 2. In addition, the permeability was compared with the value estimated by the Kozeny–Carman equation, assuming laminar flow,

$$\kappa = \left(\Phi^2 {D_p}^2/180\right)(\varepsilon^3/(1-\varepsilon)^2) \quad (9)$$

where D_p, ε, and Φ indicate the particle diameter, porosity, and sphericity, respectively. The sphericity Φ is defined as $\Phi = S_s/S_p$, where S_p and S_s represent the surface area of the particle (cylinder) and those of a sphere which has the same volume as the particle, respectively. Both permeability values agree well, indicating that the conditions including the cell size and mesh density in the micro-scale model are valid for estimating permeability.

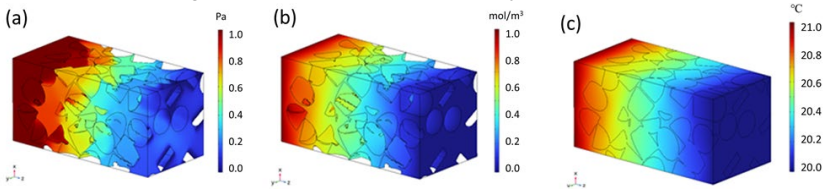

Figure 3. (a) Pressure, (b) concentration and (c) temperature distributions in sphere-packed micro-scale model.

Table 2. Geometry parameters and estimated permeability in cylinder-packed structure.

	Volume fraction (-)	Specific surface area (1/m)	Permeability (m^2)
Micro-scale model	0.498	838	1.13×10^{-8}
Kozeny–Carman eq.			1.19×10^{-8}

The effective thermal conductivity and the effective diffusion coefficient in each gas species, are shown in Table 3. For comparison, we also estimated both values based on Bruggeman's equation

$$k_{eff} = k_1\varepsilon^n, \quad D_{eff,i} = D_{0,i}\varepsilon^n \quad (10)$$

where k_1 and D_0 indicate the bulk thermal conductivity and diffusion coefficient, and n means the constant (1.5 was assumed in this study). The values estimated by the micro-scale model are close to those estimated by eq. (10), whereas the effective thermal conductivity of the micro-scale model is slightly larger. This indicates that the conditions in the micro-scale model are valid not only for the permeability but also the effective thermal conductivity and diffusion coefficients.

Table 3. Estimated effective thermal conductivities and diffusion coefficients.

	k_{eff} [W/(m²s)]	$D_{eff,i}$ [m²/s]		
		H_2	O_2	CH_3OH
Micro-scale model	0.133	4.91×10^{-5}	1.09×10^{-5}	4.67×10^{-6}
Bruggeman	0.165	5.35×10^{-5}	1.19×10^{-5}	5.09×10^{-6}

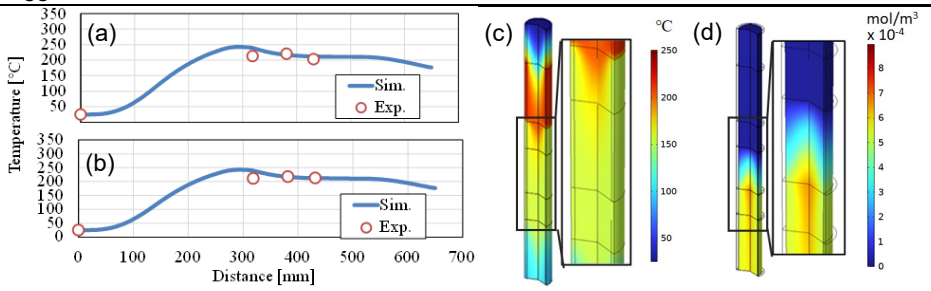

Figure 4. Comparison of temperature distribution in (a) cold case and (b) methanol synthesis, (c) simulated temperature, (d) CH_3OH concentration.

The 2D axial symmetric homogeneous model (macro-scale model) was validated to the experimental results of the cold case (without reaction) and the methanol synthesis. In the simulation, the micro-scale parameters (the effective thermal conductivity, permeability, and effective diffusion coefficient) of the cylinder shape pellet estimated in the previous section were adopted. Figure 4a and b describes the comparison of temperature between the experiment and the simulation in the cold case and the case with methanol synthesis, respectively. The simulated values agree well with the experimental ones, indicating that the macro-scale model reproduces not only the cold case but also the methanol synthesis results. In addition, the CH_3OH concentration was measured, and the value agreed well with the simulated one (simulation:5.94 $x10^{-4}$ mol/m^3, experiment:6.0$x10^{-}$

^{4} mol/m^3). Figure 4c and d shows the simulated steady-state temperature and CH_3OH concentration distribution in the reactor. The temperature increases from the reactor inlet to the catalyst layer due to the heater around the reactor and the heat generation of the catalyst layer. The concentration increases downstream of the catalyst layer. Note that the concentration is higher in the centre than near the wall. This indicates that the higher flow velocity induces the reaction of methanol synthesis in this region. These results are similar to the trends of previously reported 2-D homogenization models (Adji et al., 2019).

3.2 Effects of pellet shape on conversion

In order to clarify the effects of the pellet shape on the micro-scale parameters with the random packed sphere and hollow cylinder structures were carried out. The estimated values of volume fraction, surface area, permeability is shown in Table 4. The volume fractions of the cylinder and sphere pellets are almost 50%, whereas that of the hollow cylinder reduces to 39 % due to the hollow space in the cylinder. The specific surface area of the hollow cylinder is about 50 % larger than those of the cylinder and sphere for this reason. It should be noted that the sphere structure estimated from the micro-scale model had the highest permeability, although those estimated from the Kozeny–Carman eq. ranked between the cylinder and the hollow cylinder. This could be attributed to the sphere-packed structure having a larger average pore size and smaller tortuosity than other structures (Fu et al., 2021; Ahn et al., 2021). Table 5 shows the effective thermal conductivity in the gas phase and pellet layer, and the effective diffusion coefficient in each gas species estimated from the micro-scale model. In contrast to the permeability, the values of the hollow cylinder are higher than those of the cylinder and sphere. The effective values estimated by Bruggeman's eq. show the same tendency as those of the micro-scale model. This suggests that the porosity of the pellet region could be a dominant factor regardless of the pellet shape.

Table 4. Geometry parameters and estimated micro-scale parameters in each structure.

		Volume fraction (-)	Specific surface area (1/m)	Permeability [(m^2)
Cylinder (reshown)	Micro-scale model	0.518	943	1.13×10^{-8}
	Kozeny–Carman			1.19×10^{-8}
Sphere	Micro-scale model	0.498	838	1.36×10^{-8}
	Kozeny–Carman			9.80×10^{-9}
Hollow cylinder	Micro-scale model	0.386	1260	1.28×10^{-8}
	Kozeny–Carman			5.05×10^{-9}

Table 5. Estimated effective thermal conductivities and diffusion coefficients in each structure.

		k_{eff} (W/(m^{2}s))	$D_{eff,i}$ (m^2/s)		
		Gas	H_2	O_2	CH_3OH
Cylinder (reshown)	Micro-scale model	0.133	4.91×10^{-5}	1.09×10^{-5}	4.67×10^{-6}
	Bruggeman	0.165	5.35×10^{-5}	1.19×10^{-5}	5.09×10^{-6}
Sphere	Micro-scale model	0.138	5.47×10^{-5}	1.22×10^{-5}	5.20×10^{-6}
	Bruggeman	0.144	5.69×10^{-5}	1.27×10^{-5}	5.41×10^{-6}
Hollow cylinder	Micro-scale model	0.151	5.50×10^{-5}	1.22×10^{-5}	5.23×10^{-6}
	Bruggeman	0.211	7.70×10^{-5}	1.71×10^{-5}	7.31×10^{-6}

The 2D axial symmetric micro-scale simulations with various pellet shapes, including spheres, cylinders, and hollow cylinders, have been carried out and their performances were compared. The simulation conditions, including inlet pressure and gas concentration, were the same as in the actual experiment described in 3.1.
Figure 5a shows the profile of the gas velocity magnitude on the axial lines in each structure. The difference of the gas velocity in each pellet shape in the catalyst bed layer was only within 1%, indicating that the outlet pressure loss could determine the velocity field in the reactor. Figure 5b show the simulated temperature on the axial lines. In all structures, the temperature rises from the periphery from the inlet to the catalyst bed region and slightly decreases beyond the catalyst bed region. The temperature distribution of the cylinder pellet structure is higher than that of the other structures, with a maximum difference of about 5 °C in the catalyst bed region. It is natural to assume that this is due to the effect of effective thermal conductivity evaluated in Section 3.1. The steady-state CH_3OH concentration on the central axial are described in Fig5c. The concentration is higher near the central axis, and it increases with the distance from the inlet. In this simulation condition, the generation of CH_3OH is largest in the hollow-cylinder-shaped pellets, followed by the cylinder- and the sphere-shaped ones. This order agrees with that of the specific surface area of the pellets (Table 4), suggesting that the pellet surface area in the catalyst bed layer is the dominant factor of CH_3OH generation in the conditions, compared to permeability, thermal conductivity, and diffusion coefficient. It should be noted that these results

can vary greatly depending on conditions such as temperature, pressure, and reactor geometry. However, the present model is significant in that they enable prediction of macroscopic information such as temperature, flow velocity, and methanol concentration in the reactor from microscopic information such as pellet shape.

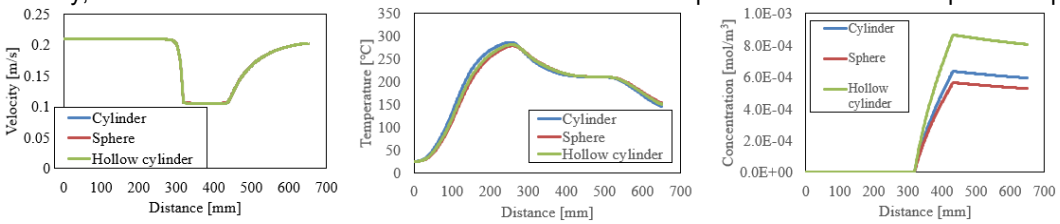

Figure 5. (a) Gas velocity, (b) temperature, (c) CH_3OH concentration in each pellet shape.

4. Conclusions

A stepwise multiscale model was developed in order to perform the homogeneous simulation of the fixed-bed reactor of CO_2 methanation considering the effect of 3D packed pellet geometry. The microscopic parameters including permeability, effective thermal conductivity, and effective diffusion coefficient were found to be in good agreement with the values estimated by the deductive equations. A macro-scale model for methanol synthesis in a fixed-bed reactor was validated using the condition of the cylindrical pellets of $Zn.Al_2O_3$ with the actual experiment. The effects of pellet shapes, including spheres and hollow cylinders, on the reactor performance were studied, and the results showed that the highest methanol reactivity was obtained for the hollow cylinder pellets, which have the largest surface area, rather than the cylindrical pellets, which have the highest permeability and thermal conductivity. While the results may be influenced by factors including temperature, pressure, and the reactor design, the importance of the present model lies in its ability to predict the reactions based on the pellet geometry. As a future research, it is proposed to extend and apply this model to other pellet shapes such as cubes and cross webs, and to conduct prediction and verification of their characteristics.

References

Adji B.S., Muharam Y., Kartohardjono, 2019, S. Simulation of Methanol Synthesis from CO2 Hydrogenation in a Packed Bed Reactor Using COMSOL Multiphysics, International Journal of Engineering Research and Technology,12, 12, 2592-2599.

Ahn J., Kim H., Ro Y., Kim J., Chung W., Chang S., 2021, Development of Pilot-Scale CO2 Methanation Using Pellet-Type Catalysts for CO2 Recycling in Sewage Treatment Plants and Its Validation through Computational Fluid Dynamics (CFD) Modeling. Catalysts 11, 1005.

Alarcón A., Busqué R., Andreu T., Guilera J., 2022, Design of a Multi-Tubular Catalytic Reactor Assisted by CFD Based on Free-Convection Heat-Management for Decentralised Synthetic Methane Production. Catalysts, 12, 1053.

An Q., On Application of Computer Simulation Technology in Methanol Synthesis in the Coal Chemical Industry, 2017, Chemical Engineering Transactions 59, 607-612.

Fu J., Hywel R. T., Li C., 2021, Tortuosity of Porous Media: Image Analysis and Physical Simulation. Earth-Science Reviews 2021, 212, 103439.

Kato Y., 2010, Carbon Recycling for Reduction of Carbon Dioxide Emission from Iron-Making Process. ISIJ International, 50, 181–185.

Maestri M., Cuoci A., 2013, Coupling CFD with detailed microkinetic modelling in heterogeneous catalysis, Chemical Engineering Science 96, 106.

Shahrokhi M. and Baghmisheh G.R., 2005, Modeling, simulation and control of a methanol synthesisfixed-bed reactor, Chemical Engineering Science 60, 4275.

Son M., Woo Y., Kwak G., Lee Y. J., Park M. J., 2019, CFD modeling of a compact reactor for methanol synthesis: Maximizing productivity with increased thermal controllability, International Journal of Heat and Mass Transfer 145, 118776.

Taco-Vasquez S., Ron C.A., Murillo H.A., Chico A., Arauz P.G., 2022, Thermochemical Analysis of a Packed-Bed Reactor Using Finite Elements with FlexPDE and COMSOL Multiphysics. Processes, 10, 1144.

Zhang X., Zhang G, Song C., Guo X., 2021, Catalytic Conversion of Carbon Dioxide to Methanol: Current Status and Future Perspective. Frontiers in Energy Research 8, 621119.